ELSEVIER

Earth and Planetary Science Letters 192 (2001) 507–521

EPSL

www.elsevier.com/locate/epsl

The kinematic evolution of the Nepalese Himalaya interpreted from Nd isotopes

Delores M. Robinson [a,*], Peter G. DeCelles [a], P. Jonathan Patchett [a], Carmala N. Garzione [b]

[a] *Department of Geosciences, University of Arizona, Tucson, AZ 85721, USA*
[b] *Department of Earth Sciences, University of Rochester, Rochester, NY 14627, USA*

Received 17 April 2001; received in revised form 16 July 2001; accepted 17 July 2001

Abstract

Neodymium (Nd) isotopes from the Himalayan fold-thrust belt and its associated foreland basin deposits are useful for distinguishing between Himalayan tectonostratigraphic zones and revealing the erosional unroofing history as controlled by the kinematic development of the orogen. Neodymium isotopic data from the Himalayan fold-thrust belt in Nepal ($n=35$) reveal that the Lesser Himalayan zone consistently has a more negative $\varepsilon_{Nd}(0)$ value than the Greater and Tibetan Himalayan zones. Our data show the average $\varepsilon_{Nd}(0)$ value in the Lesser Himalayan zone is -21.5, whereas the Greater and Tibetan Himalayan zones have an average $\varepsilon_{Nd}(0)$ value of -16. These consistently distinct values throughout Nepal enable the use of Nd isotopes as a technique for distinguishing between Lesser Himalayan zone and Greater Himalayan zone rock. The less negative $\varepsilon_{Nd}(0)$ values of the Greater Himalayan rocks support the idea that the Greater Himalayan zone is not Indian basement, but rather a terrane that accreted onto India during Early Paleozoic time. Neodymium isotopic data from Eocene through Pliocene foreland basin deposits ($n=34$) show that sediment provenance has been dominated by Greater and Tibetan Himalayan detritus across Nepal. The $\varepsilon_{Nd}(T)$ values in the synorogenic rocks in western and central Nepal generally show an up-section shift toward more negative values and record the progressive unroofing of the different tectonostratigraphic zones. At $\sim$10 Ma in Khutia Khola and $\sim$11 Ma in Surai Khola, a shift in $\varepsilon_{Nd}(T)$ values from -16 to -18 marks the erosional breaching of a large duplex in the northern part of the Lesser Himalayan zone. This shift is not seen in eastern Nepal, where the $\varepsilon_{Nd}(T)$ values remain close to -16 throughout Miocene time because there has been less erosional unroofing in this region.

Keywords: Nd-144/Nd-143; Himalayas; Nepal; provenance

1. Introduction

The Himalayan fold-thrust belt is composed of four tectonostratigraphic terranes that are continuous along strike for a distance of $\sim$2300 km from northern Pakistan to the Namche Barwa syntaxis [1]. These are, from north to south, the Tibetan, Greater, and Lesser Himalayan zones

* Corresponding author. Tel.: +1-520-621-6020; Fax: +1-520-621-2672.
E-mail addresses: dmr@geo.arizona.edu (D.M. Robinson), decelles@geo.arizona.edu (P.G. DeCelles), patchett@geo.arizona.edu (P.J. Patchett), garzione@siena.earth.rochester.edu (C.N. Garzione).

0012-821X/01/$ – see front matter
PII: S0012-821X(01)00451-4

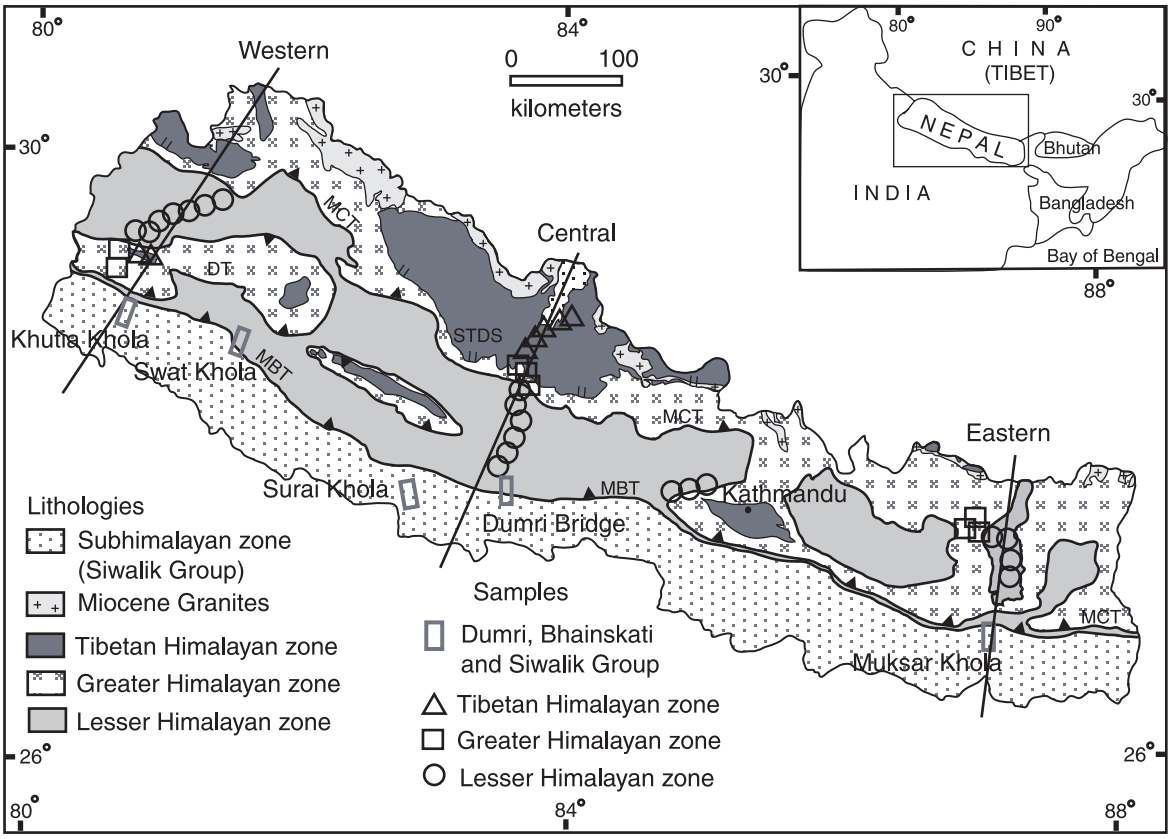

Fig. 1. Generalized geologic map of Nepal, showing major thrust faults (barbed lines), normal faults (double-ticked lines), and tectonostratigraphic terranes. MBT, Main Boundary thrust; MCT, Main Central thrust; DT, Dadeldhura thrust (a Greater Himalayan klippe); STDS, South Tibetan Detachment system. Lines labeled western, central, and eastern indicate schematic cross-sections shown in Fig. 6.

and Subhimalayan zone (Fig. 1). These terranes are lithologically and petrologically distinctive, and thus, many studies have utilized modal petrographic data to determine the erosional unroofing history of the orogenic belt and to develop kinematic sequences of thrust sheet emplacement [2–8]. Although these studies reveal reasonably consistent results, the fact that similar lithologies likely to generate sandy clastic detritus upon weathering, such as quartzite and coarse-grained quartzo-feldspathic igneous rocks, are present in several of the Himalayan terranes renders conventional petrographic studies somewhat equivocal when it comes to proving specific source terranes. Ideally, modal petrographic data should be complemented by strategically sampled geochemical data [9–11]. This approach is especially applicable to the Himalaya because several previous studies have documented major differences between the Nd isotopic signatures and detrital U–Pb zircon ages of two of the most important of these terranes – the Lesser and Greater Himalayan zones [12–16].

The previous isotopic studies of the Himalayas were undertaken in restricted areas in Pakistan [13], northern India [16] and a small area in central Nepal [12]. A regional, along-strike data set is needed to confirm the continuity of the patterns suggested in these previous studies. In this paper we present the results of Nd isotopic analyses of all of the Himalayan terranes throughout Nepal from three >200 km long foot traverses that span an ~ 800 km wide region. In addition, we utilize the Nd isotopic

compositions of paleontologically and magnetostratigraphically dated Eocene–Pliocene foreland basin deposits to assess the erosional unroofing history of the orogenic belt. Our results confirm the previous isotopic studies (with some modifications) of Himalayan terranes and require a tectonic explanation of the major differences between Lesser and Greater Himalayan isotopic compositions. In addition, a systematic erosional unroofing history of the orogen is preserved in the Nd isotopic compositions of the foreland basin deposits.

Greater Himalayan Zone

Formation III	Garnet-tourmaline augen orthogneiss, migmatitic quartzo-feldspathic sillimanite-bearing schist, and calc-silicate gneiss	ca. 480-500 Ma [12,14,15]
Formation II	Diopside-garnet-amphibole-bearing cal-silicate gneiss and marble	
Formation I	Kyanite-garnet bearing pelitic gneiss and migmatite, abundant quartzite	ca. 830 Ma [12,14,15]

Lesser Himalayan Zone

Age	Western Nepal [30]	Central Nepal [29]	Eastern Nepal (modified from [23])
Miocene	Dumri Fm.	Dumri Fm.	Dumri Fm.
Eocene	Bhainskati Fm	Bhainskati Fm	Bhainskati Fm
Cretaceous-Permian	Gondwanas	Gondwanas	Gondwanas
Middle Proterozoic	Lakaparta Gr. (including Benighat slate)	Robang Fm. Malekhu Fm. Benighat Fm. Dhading Fm.	Tumlingtar Group (including Ulleri Augen Gneiss, 1.83 Ga)
	Syangia Fm	Norpul Fm.	
	Galyang Fm.	Dandagaon Fm.	
	Sangram Fm. <1.68 Ga	Fagfog Fm.	
Early Proterozoic	1.86-1.83 Ga: Ranimata Fm. (including Ulleri Augen Gneiss)	Kuncha Fm. (including Ulleri Augen Gneiss)	
	1.86-1.83 Ga: Kushma Fm.		

Fig. 2. Stratigraphy of the Lesser and Greater Himalayan zones. The Greater Himalayan nomenclature was principally developed by LeFort [21].

2. Regional geologic setting

2.1. Tectonostratigraphy of Nepal and southern Tibet

The Himalayan orogen comprises four distinct tectonostratigraphic units. The northernmost zone is the Tibetan Himalayan zone which is ca. 50–25 Ma fold-thrust belt composed of Cambrian to Eocene sedimentary rocks. It is ~200 km wide and has a stratigraphic thickness of 10 km [17] (Fig. 1). The stratigraphic succession of this zone is referred to as the Tethyan sequence. The South Tibetan Detachment system, a family of normal faults that activated ca. 23–20 Ma [18–20], separates the Tibetan Himalayan zone from the Greater Himalayan zone to the south.

The Greater Himalayan zone is composed of paragneiss, orthogneiss, amphibolite, schist, calc-silicates, marble, and metavolvanics and may be divided into three informal formations [21,22] (Fig. 2). The Greater Himalayan zone consistently dips northward and may be up to 20 km thick [23]. Detrital zircon U–Pb ages reveal a maximum age of 830 Ma and intruding granites yield a minimum age of ~480 Ma [12,14,15]. Several isolated synformal klippen south of the Greater Himalayan zone consist of schist, metavolcanics, gneiss, and Paleozoic sedimentary rocks. These include the Dadeldhura, Karnali, Kathmandu, and Jarjarkot klippen. The metamorphic rocks in the klippen are thought to be related to the Greater Himalayan zone [24]. The unmetamorphosed sedimentary rocks in the klippen are similar to the Tethyan sequence of the Tibetan Himalayan zone. The Greater Himalayan zone is separated from the Lesser Himalayan zone by the Main Central thrust, which was active beginning ca. 23–20 Ma [25–28].

The Lesser Himalayan zone is composed of unmetamorphosed to greenschist facies sedimentary rocks with a stratigraphic thickness of ~10 km [29,30]. Rocks in the lower Lesser Himalayan sequence (Fig. 2; Kushma, Ranimata, Ulleri and equivalents) are Paleo- and Meso-Proterozoic in age (1.86–1.83 Ga; [14,15]). The Sangram Formation contains zircons that are as young as 1.68 Ga [14,15]. Algal stromatolites in the Lakaparta Group suggest a Proterozoic age [31]. The remaining upper portion of the Lesser Himalayan zone is composed of the Permian to Paleocene Gondwanas, the Eocene Bhainskati Formation, and the Early Miocene Dumri Formation [32]. We use the nomenclature for the stratigraphy from western Nepal for the equivalent formations across Nepal (Fig. 2). The Lesser Himalayan zone contains a complex series of thrust sheets and a hinterland-dipping duplex north of the synformal Greater Himalayan klippen and an imbricated zone to the south of the klippen. The Lesser Himalayan zone is separated from the Subhimalayan zone to the south by the Main Boundary thrust, which was active in Middle–Late Miocene time [30].

The Subhimalayan zone consists of the Siwalik Group and contains the <14 Ma synorogenic rocks shed from the fold-thrust belt. The Siwalik Group ranges in stratigraphic thickness from 3.5 to 5.5 km and contains informal lower, middle, and upper members. The members are imbricated into two or three southward directed and northward-dipping thrust sheets. The active southernmost thrust is usually expressed as an anticline at the surface and delineates the Main Frontal thrust [33–35].

2.2. Previous Nd isotopic results

Previous studies have documented Nd isotopic compositions of Himalayan rocks in central Nepal, India, and Pakistan. The $\varepsilon_{Nd}(0)$ values obtained are as follows: -17 to -11 in the Tethyan sequence ([16] and references therein), -19 to -5 in the Greater Himalayan sequence [12,13,16,36–39] and -28 to -15 in the Lesser Himalayan sequence [12,16,40]. Samples from the lower Lesser Himalayan sequence (Ranimata Formation and its stratigraphic equivalents) have $\varepsilon_{Nd}(0)$ values ranging from -28 to -21. Samples from the upper Lesser Himalayan sequence (Sangram, Galyang, and Syangia Formations and the Lakaparta Group and their stratigraphic equivalents) yield $\varepsilon_{Nd}(0)$ values between -25 and -16. No previous Nd isotopic studies have been conducted in the Subhimalayan zone.

Historically, the Lesser and Tethyan Himalayan

Table 1
Bedrock samples

Sample	Rock type	Formation	Location	Age (Ma)	Sm (ppm)[c]	Nd (ppm)[c]	$^{147}Sm/^{144}Nd$[b]	$^{143}Nd/^{144}Nd$	±2σ	$\varepsilon_{Nd}(0)$[d]	T_{DM} (Ma)
Tibetan Himalayan zone											
1TBkag	sandstone	Chukh Fm	central	100	16.50	84.95	0.1174	0.512322	31	−6.2	1142
2TBpha	shale	Dogger Fm	central	200	4.75	33.22	0.0864	0.511805	15	−16.2	1479
3TBjom	shale	Jomson Fm	central	180	9.05	53.17	0.1028	0.511673	12	−18.8	1881
4TBSya	phyllite	Tilicho Fm	central	400	10.35	63.38	0.0987	0.511671	9	−18.9	1816
5TBMar	phyllite	Tilichio Fm	central	400	11.80	64.50	0.1105	0.51175	11	−17.3	1908
DD-31	shale	Melmura Fm	far western	400	5.84	29.59	0.1193	0.511734	7	−17.6	2114
DD-33	shale	Melmura Fm	far western	400	6.71	35.99	0.1128	0.51161	9	−20.1	2166
Greater Himalayan zone											
AG-106	paragneiss	Formation I	eastern	800	6.48	35.16	0.1113	0.511619	10	−19.9	2121
AG-109	paragneiss	Formation I	eastern	800	6.97	38.69	0.1089	0.511714	14	−18.0	1930
9TBkal	orthogneiss	Formation III	central	800	7.08	27.92	0.1533	0.512137	30	−9.8	2289[a]
12TBgh	paragneiss	Formation I	central	800	7.26	37.85	0.1160	0.511814	13	−16.1	1914
13TBru	paragneiss	Formation II	central	800	8.36	41.77	0.1209	0.511946	14	−13.5	1798
AG-105	paragneiss	Formation I	eastern	800	2.17	8.85	0.1483	0.511836	14	−15.6	2845[a]
Greater Himalayan klippen											
DDG-98	granite	C-O granite, DT	far western	492	6.02	26.60	0.1369	0.512034	15	−11.8	1998[a]
DD-40	schist	Kalikot Schist, Dt	far western	500	3.88	18.74	0.1250	0.512248	7	−7.6	1361
Lesser Himalayan zone											
K1-99	shale	Benighat Fm	central	1600	3.97	29.93	0.0801	0.511343	14	−25.3	1939
SR-37	shale	Benighat Fm	far western	1600	3.83	20.00	0.1159	0.51163	12	−19.7	2205
SR-35	shale	Benighat Fm	far western	1600	5.05	27.79	0.1098	0.511575	11	−20.7	2156
DD-58	shale	Benighat Fm	far western	1600	7.37	42.22	0.1055	0.51143	11	−23.6	2277
23TBtu	shale	Syangia Fm	central	1600	5.82	33.15	0.1062	0.51163	26	−19.7	2003
23TBSe	phyllite	Syangia Fm	central	1600	6.23	37.03	0.1016	0.511339	11	−25.3	2323
CH-1	phyllite	Galyang Fm	far western	1600	3.04	16.16	0.1138	0.51146	15	−23.0	2424
DD-15	phyllite	Galyang Fm	far western	1600	10.10	52.32	0.1167	0.511741	25	−17.5	2045
22TBPu	shale	Galyang Fm	central	1600	7.36	37.77	0.1177	0.511711	13	−18.1	2116
24TBLi	phyllite	Galyang Fm	central	1600	10.98	65.18	0.1018	0.511521	11	−21.8	2074
K3-99	shale	Galyang Fm	central	1600	3.57	18.42	0.1170	0.511557	9	−21.1	2349
DD-52	shale	Sangram Fm	far western	1600	9.31	49.94	0.1127	0.511822	12	−15.9	1839
20TBSI	shale	Sangram Fm	central	1600	8.72	47.63	0.1107	0.511444	8	−23.3	2374
18TBBra	shale	Ranimata Fm	central	1870	6.70	38.76	0.1044	0.511333	42	−25.5	2393
K2-99	phyllite	Ranimata Fm	central	1870	6.62	34.82	0.1148	0.511369	15	−24.2	2553
AG-103	phyllite	Ranimata Fm	eastern	1870	6.75	35.31	0.1155	0.511518	10	−21.9	2376
AG-104	phyllite	Ranimata Fm	eastern	1870	3.90	21.22	0.1112	0.51137	12	−24.7	2499
SR-30	gneiss	Ulleri	far western	1850	5.26	25.11	0.1266	0.511647	8	−19.3	2455
AG-111	gneiss	Ulleri	eastern	1850	4.82	21.96	0.1327	0.511652	14	−19.2	2636[a]
AG-112	gneiss	Ulleri	eastern	1850	5.15	25.72	0.1210	0.511571	11	−20.8	2430

[a] Unrealistic model age probably due to elevated Sm/Nd ratio.
[b] 2σ reproducibilities of 0.4%.
[c] 2σ reproducibilities of 1%.
[d] Error in ε_{Nd} varies between 0.1 and 0.6 epsilon units, for young samples it is a function of the error in $^{143}Nd/^{144}Nd$. 18TBBra has an error of 0.8 epsilon units.

sequences are considered to be composed of sediments shed from the Indian craton, and the Greater Himalayan sequence is considered to be Indian cratonic basement. Several recent Nd isotopic studies, however, suggest that the Greater Himalayan rocks are not Indian basement [12,13,16]. Sediments derived from an old craton will record its characteristic negative $\varepsilon_{Nd}(0)$ values [9,41]. Therefore, the miogeoclinal and basement rocks in the fold-thrust belt should yield the same

isotopic characteristics of the Indian craton if they were derived from that craton. The Indian craton consists of Archean and Early Proterozoic metamorphic rocks [42] that have very negative $\varepsilon_{Nd}(0)$ values [43]. Rocks of the Lesser Himalayan zone are characterized by highly negative $\varepsilon_{Nd}(0)$ values, consistent with sedimentary rocks derived from the Indian craton. Rocks of the Greater Himalayan zone, by contrast, have $\varepsilon_{Nd}(0)$ values much less negative than those of the Indian craton. In addition, U–Pb detrital zircon ages from the Greater Himalayan sequence suggest that it is

Table 2
Synorogenic foreland basin samples

Sample	member	Age (Ma)	Sm (ppm)[b]	Nd (ppm)[b]	$^{147}Sm/^{144}Nd$[a]	$^{143}Nd/^{144}Nd$	±2σ	$\varepsilon_{Nd}(T)$[c]	T_{DM} (Ma)
Khutia Khola–western Nepal									
KK30ps	lower	12	7.14	36.75	0.1174	0.511882	7	−14.6	18.34
KK179ps	lower	11.5	8.17	43.92	0.1125	0.511822	11	−15.8	1835
KK437ps	lower	11	6.26	32.49	0.1165	0.511841	11	−15.4	1882
KK730ps	lower	10.5	7.17	37.80	0.1147	0.511843	6	−15.4	1845
KK1234	middle	9	7.41	40.09	0.1117	0.511763	6	−17.0	1911
KK1465ps	middle	8.5	6.67	34.40	0.1170	0.511723	7	−17.8	2084
KK2947ps	middle	5	6.94	36.07	0.1164	0.511748	7	−17.3	2027
KK3292	upper	4	7.47	39.32	0.1149	0.511859	11	−15.2	1823
KK3330	upper	4	7.01	36.75	0.1152	0.511852	10	−15.3	1840
Surai Khola–central Nepal									
SK87	lower	11.5	7.01	35.70	0.1188	0.511794	7	−16.4	2004
SK79	lower	11	5.45	26.22	0.1256	0.511838	11	−15.5	2083
SK91	middle	8	6.07	30.70	0.1196	0.511727	6	−17.7	2132
SK95	middle	5.5	6.34	32.64	0.1174	0.511795	8	−16.4	1973
SK114	middle	4	7.77	40.69	0.1154	0.511839	23	−15.5	1863
SK110	upper	2	5.37	28.04	0.1159	0.511715	9	−18.0	2068
SK98	upper	1	6.14	31.93	0.1162	0.511789	7	−16.5	1959
SK72	upper	1	7.18	37.27	0.1164	0.511814	11	−16.1	1922
Muksar Khola–eastern Nepal									
GK67	lower	10	7.92	42.27	0.1133	0.511813	8	−16.0	1864
GK395	middle	9	7.98	41.10	0.1174	0.511808	8	−16.1	1952
GK651	middle	9	6.86	33.78	0.1228	0.511805	13	−16.2	2076
GK835	middle	8	8.06	41.52	0.1173	0.511773	12	−16.8	2007
GK1085	middle	8	7.81	41.03	0.1150	0.511779	8	−16.7	1951
GK1377	middle	7	8.88	43.21	0.1242	0.511843	24	−15.4	2042
GK1782	middle	6	7.57	39.46	0.1159	0.511807	9	−16.1	1924
GK2531	middle	5	8.10	42.08	0.1164	0.511813	9	−16.0	1924
GKUS4	upper	4	8.24	42.78	0.1165	0.511821	14	−15.9	1913
GKUS5	upper	4	8.46	43.34	0.1180	0.51183	8	−15.7	1930
Swat Khola									
ST497	697 m	20	7.08	36.71	0.1167	0.511902	6	−14.2	1788
ST627	827 m	18	7.61	38.70	0.1188	0.511885	7	−14.5	1857
ST997	1197 m	17	6.86	36.52	0.1135	0.511918	7	−13.9	1708
SKT	1397 m	15	7.26	36.48	0.1204	0.511957	6	−13.1	1769
Dumri Bridge									
Bal-28-96	10 m	45	7.22	35.13	0.1242	0.512199	14	−8.1	1433
DB0.1	100 m	42	9.25	46.62	0.1199	0.512067	5	−10.7	1581
DB11P	200 m	25	9.22	47.24	0.1180	0.511859	6	−14.9	1883
Modern river sediment									
TR11	0	0	6.09	31.35	0.1174	0.51173	9	−17.7	2078

[a] 2σ reproducibilities of 0.4%.
[b] 2σ reproducibilities of 1%.
[c] Error in Nd varies between 0.1 and 0.5 epsilon units, for young samples it is a function of the error in $^{143}Nd/^{144}Nd$.

much younger than the Lesser Himalayan sequence [12,14,15]. Thus, the rocks of the Greater Himalayan zone are probably not Indian cratonic basement but are likely an exotic terrane that accreted onto India during Early Paleozoic time [15].

3. Methods

Bedrock samples were collected along regional foot traverses along the Seti River in western Nepal, the Kali Gandaki in central Nepal, and the Arun River in eastern Nepal. These major river drainages served as inlets into the core of the mountain belt allowing us to continuously collect samples while mapping wide swaths of territory. The stratigraphic and structural frameworks of the samples are, therefore, well characterized [6,30,44]. Fine-grained shales, slates, and phyllites and lithologically homogeneous rock from the Lesser and Tibetan Himalayan zones were sampled. Large samples of the finest-grained paragneiss and orthogneiss were collected from the Greater Himalayan zone. Siltstones in the Subhimalayan zone were sampled at three locations south of the three transects at Khutia Khola, Surai Khola, and Muksar Khola. These samples were collected from detailed measured sections [6,45] in conjunction with magnetostratigraphic studies which established the age of each sample [46]. Samples from the synorogenic Dumri and Bhainskati Formations were collected at Swat Khola and the Dumri Bridge area, also in the context of detailed measured sections [5]. The age of the Dumri Formation is known from paleomagnetic stratigraphy (T.P. Ojha, personal communication) and detrital muscovite $^{40}Ar/^{39}Ar$ ages that indicate the unit must be younger than $\sim$22 Ma [7,30]. The age of the Bhainskati Formation is known from detailed biostratigraphy [32].

Isotopic analyses were determined on a Thermal Ionization Mass Spectrometer (TIMS) at the University of Arizona. Samples were powdered to less than 200 mesh in an alumina shatter box. 300 mg samples were digested for 1 week in Hf–HNO_3 in high-pressure teflon bomb vessels at 160°C. The samples were dried down and then heated overnight in orthoboric acid and then dried down completely. After further HCl treatments, separation of Sm and Nd was performed by standard techniques [47]. Nd isotopic measurements were fractionation-corrected to $^{146}Nd/^{144}Nd = 0.7219$. Table 1 contains the data from the bedrock samples (calculated at time $T = 0$). Table 2 contains the data from the synorogenic sediments with initial $\varepsilon_{Nd}(T)$ values calculated at the time of sedimentation. Depleted mantle model ages were calculated based on the model of DePaolo [48]. We list Nd model ages but do not employ them in the discussion because mixed provenance can render model ages for sediments very misleading [49]. The La Jolla Nd isotopic standard gave $^{143}Nd/^{144}Nd = 0.511868$ with one standard deviation of 0.000008 based on 10 runs.

4. Results

The $\varepsilon_{Nd}(0)$ values determined in this study are listed in Table 1 and distinguished in terms of their different tectonostratigraphic zones in Fig. 3. The Tibetan Himalayan zone samples range in $\varepsilon_{Nd}(0)$ values from -20.1 to -6.2. The less evolved nature of sample 1TBkag (-6.2), from the Cretaceous Chukh Formation in the upper part of the Tethyan sequence, may be due in part to the presence of detrital volcanic clasts derived from the magmatic arc [50] and/or obducted ophiolites from the Indian–Eurasian collision.

Greater Himalayan paragneiss $\varepsilon_{Nd}(0)$ values range from -19.9 to -13.5, with an orthogneiss at -9.8 (9TBkal). Two samples from the Dadeldhura thrust sheet (one of the Greater Himalayan klippen) in western Nepal yielded $\varepsilon_{Nd}(0)$ values of -7.6 from the Kalikot Schist (DD-40) and -11.8 from the 492 Ma [6] Dadeldhura Granite (DDG-98).

The Lesser Himalayan zone samples produced $\varepsilon_{Nd}(0)$ values that range from -25.5 to -15.9. Samples from the lower part of the Lesser Himalayan sequence (Ranimata Formation) consistently contain the most negative values of -25.5 to -21.9. Samples from the upper Lesser Himalayan sequence (Benighat, Syangia, Galyang, and Sangram Formations) have values of -25.3 to

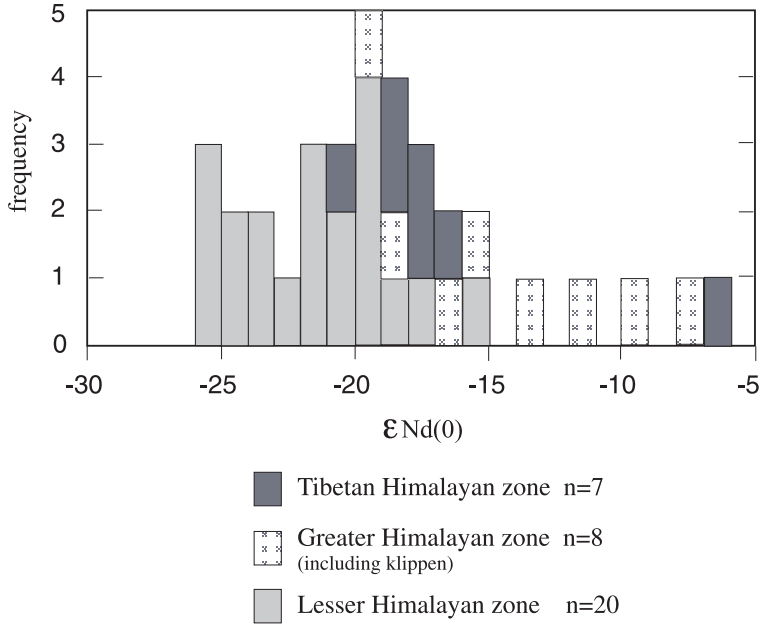

Fig. 3. $\varepsilon_{Nd}(0)$ values from the Lesser, Greater, and Tibetan Himalayan zones across Nepal. Sample sites are marked on Fig. 1.

−15.9. We observed no trend of progressively less negative values up-section in the upper Lesser Himalayan sequence as reported by Ahmad et al. [16] in Garhwal, India.

The foreland basin sequence exhibits a general up-section decrease in $\varepsilon_{Nd}(T)$ values (Fig. 4). Samples from the Eocene Bhainskati Formation (Dumri Bridge, Table 2) have $\varepsilon_{Nd}(T)$ values between −8.1 and −14.9. A major unconformity, spanning ∼15 million years, separates the Bhainskati from the overlying Early Miocene Dumri Formation [6]. Samples from the Dumri Formation (Swat Khola, Table 2) have $\varepsilon_{Nd}(T)$ values ranging from −14.5 to −13.1, and show a weak up-section trend toward less negative values (Fig. 4). Samples from Khutia Khola (Table 2) start at an $\varepsilon_{Nd}(T)$ value of −14.6 in the lower Siwalik member which was deposited beginning at 12 Ma. After ∼10 Ma, the $\varepsilon_{Nd}(T)$ values in the middle Siwalik member trend toward more negative values of approximately −18. This value seems to remain steady throughout Middle–Late Miocene time at Khutia Khola (Fig. 4) with values becoming less negative (−15.2) at 4 Ma. The average $\varepsilon_{Nd}(T)$ value is −16 for samples from Surai Khola (Table 2) in the lower Siwalik member at ∼11 Ma. One data point in the middle Siwalik member at 8 Ma has an $\varepsilon_{Nd}(T)$ value of −17.7. This suggests that a possible shift toward more negative values occurred between 11 Ma and 8 Ma. The Surai Khola section becomes less negative through Middle–Late Miocene time to −15.5 at 4 Ma, and the upper Siwalik member has values between −17.7 and −16.4. Samples from Muksar Khola (Table 2) have an $\varepsilon_{Nd}(T)$ value of −16 at 10 Ma. The values throughout Middle–Late Miocene time rarely vary from −16 with a minimum of −16.8 and a maximum of −15.4.

5. Discussion

5.1. Patterns

Tibetan Himalayan zone samples from our study have an average $\varepsilon_{Nd}(0)$ value of −16.4, and Greater Himalayan zone samples have an average $\varepsilon_{Nd}(0)$ value of −15.5. The Nd isotopic similarity of these two terranes makes it difficult to distinguish between them using Nd isotopes. Lesser Himalayan zone samples have an average $\varepsilon_{Nd}(0)$ value of −21.5. Our data (Table 1, Fig. 3)

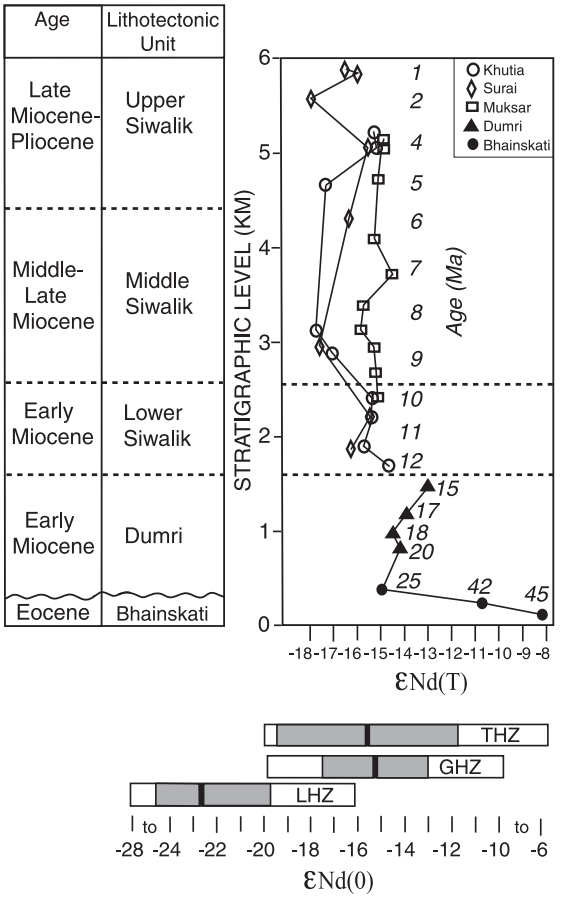

Fig. 4. $\varepsilon_{Nd}(T)$ values from the synorogenic rocks are plotted on the horizontal axis with stratigraphic thickness and corresponding time period on the vertical axis. Approximate ages (Ma) are given along the right-hand side of the figure. Along the base, the range of $\varepsilon_{Nd}(0)$ values from the different tectonostratigraphic zones from our study and previous studies ([16] and references therein) are shown with the average $\varepsilon_{Nd}(0)$ value marked with a black bar and the standard deviation of the average shown by the gray bars. For published data, the average and standard deviations are as follows: Lesser Himalayan zone (LHZ): -22.7 ± 3 ($n = 58$); Greater Himalayan zone (GHZ): -15.2 ± 2.2 ($n = 53$); Tibetan Himalayan zone (THZ): -15.6 ± 3.7 ($n = 13$). Two different scales are shown: $\varepsilon_{Nd}(0)$ values are labeled along the base of the figure corresponding to the average values, and $\varepsilon_{Nd}(T)$ values are labeled below the figure corresponding to the synorogenic rocks. Samples from the Eocene Bhainskati and Early Miocene Dumri Formations are from Swat Khola and the Dumri Bridge area in central Nepal. These values are appended to the base of the data from Khutia Khola in western Nepal, Surai Khola in central Nepal, and Muksar Khola in eastern Nepal.

show that some overlap occurs between Lesser and Greater Himalayan $\varepsilon_{Nd}(0)$ values in Nepal. However, in the context of previously published Nd isotopic data from throughout the Himalaya ([16] and references therein) which indicate a clear-cut separation between the Lesser and Greater Himalayan values, this overlap is relatively minor. In general, the Lesser Himalayan $\varepsilon_{Nd}(0)$ values are significantly more negative than $\varepsilon_{Nd}(0)$ values in the Greater and Tibetan Himalayan zones. Therefore, we conclude that Nd isotopes can be used to distinguish between rocks of the Lesser Himalayan zone and the Greater and Tibetan Himalayan zones across Nepal. This is consistent with results from Ahmad et al. [16]. The ability to differentiate between Lesser and Himalayan rocks is important in areas such as the Main Central thrust, which separates the two zones. The location of the thrust is debated because there is no clear structural discontinuity across the boundary [28,51–53]. Careful sampling for Nd isotopic studies in the context of detailed geologic mapping may help to resolve the debate about where to place the Main Central thrust in the field.

The Bhainskati and Dumri Formations show an up-section trend from $\varepsilon_{Nd}(T)$ values of -8.1 during Eocene time to -14.1 during Early–Middle Miocene time. The less negative values in the Eocene suggest the source of sediment was the upper part of the Tibetan Himalayan zone, which is characterized by less negative values. The $\varepsilon_{Nd}(T)$ values in Early Miocene time (-16) reflect the average values of the Greater/lower Tibetan Himalayan zones and thus were probably derived from these two zones (Fig. 5A). There is a shift to slightly more negative $\varepsilon_{Nd}(T)$ values of approximately -18 in the lower Siwalik member after $\sim$10 Ma in Khutia Khola and after $\sim$11 Ma in Surai Khola. We interpret the negative shift as the result of erosional breaching of a growing duplex in the Lesser Himalayan zone in the northern portion of the central and western parts of the fold-thrust belt in Nepal (Fig. 5B, C; [30]). The $\varepsilon_{Nd}(T)$ values in Muksar Khola in eastern Nepal do not show a shift toward more negative values but instead remain steady through Miocene time (-16). Thus, the $\varepsilon_{Nd}(T)$ values from the synoro-

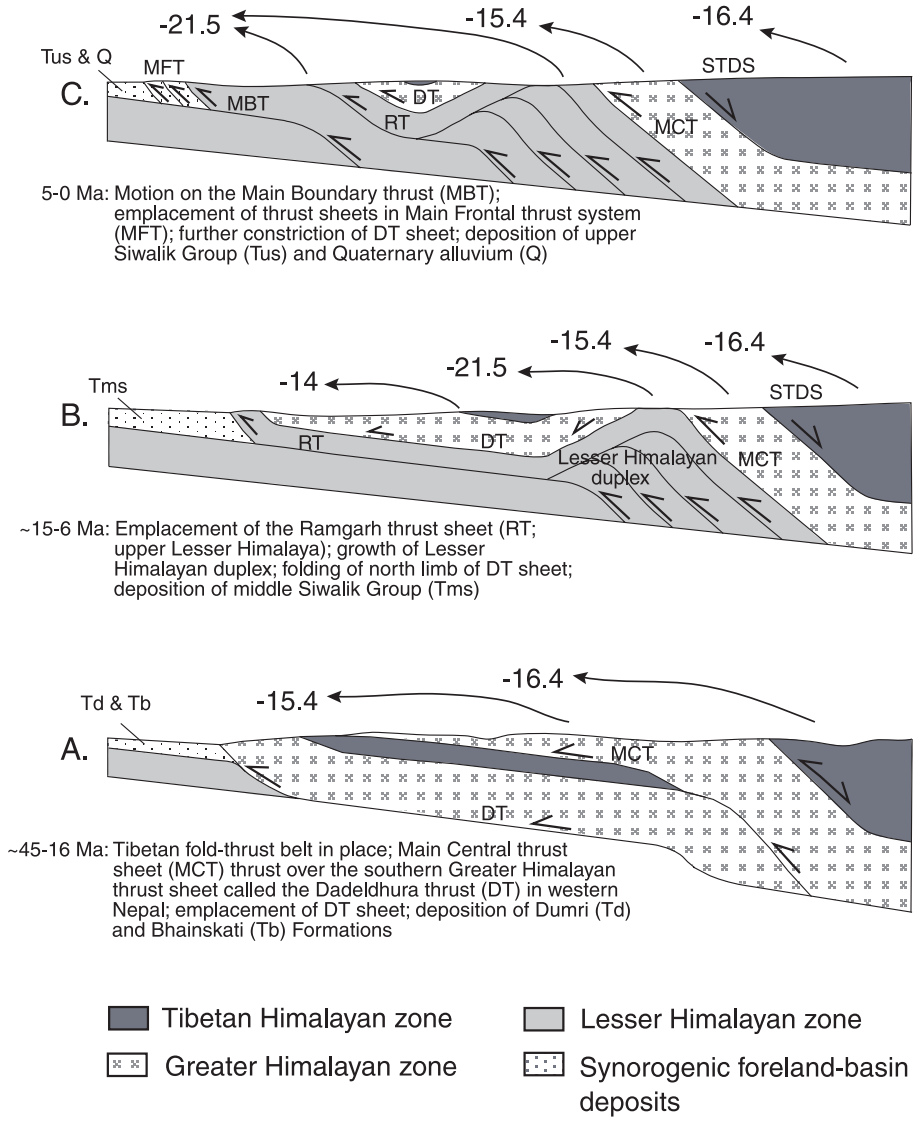

Fig. 5. Schematic reconstruction of the Himalayan fold-thrust belt in western Nepal. Abbreviations are as follows: STDS, South Tibetan Detachment system; MCT, Main Central thrust; DT, Dadeldhura thrust; RT, Ramgarh thrust; MBT, Main Boundary thrust; MFT, Main Frontal thrust; Tb, Bhainskati Formation; Td, Dumri Formation; Tsm, Tertiary middle Siwalik member; Tsu, Tertiary upper Siwalik member; Q, Quaternary alluvium. The arrows show the average $\varepsilon_{Nd}(0)$ values of the tectonostratigraphic zones (from this study only) that contributed detritus to the foreland basin deposits during each time period.

genic sedimentary rocks suggest that eastern Nepal has experienced less erosional unroofing. This is consistent with geologic mapping, which indicates that Greater Himalayan rocks still blanket the Lesser Himalayan sequence. Lesser Himalayan rock was not exposed until recently when erosion created the Arun River Gorge north of Muksar Khola and cut down into the lower Lesser Himalayan Ramgarh thrust sheet (Kushma and Ranimata Formations and equivalents). The $\varepsilon_{Nd}(T)$ values at Khutia Khola seem to remain steady at −18 through Middle–Late Miocene time but revert back to a Greater/Tibetan Himalayan signature of −15 between 5 and 4 Ma. We explain

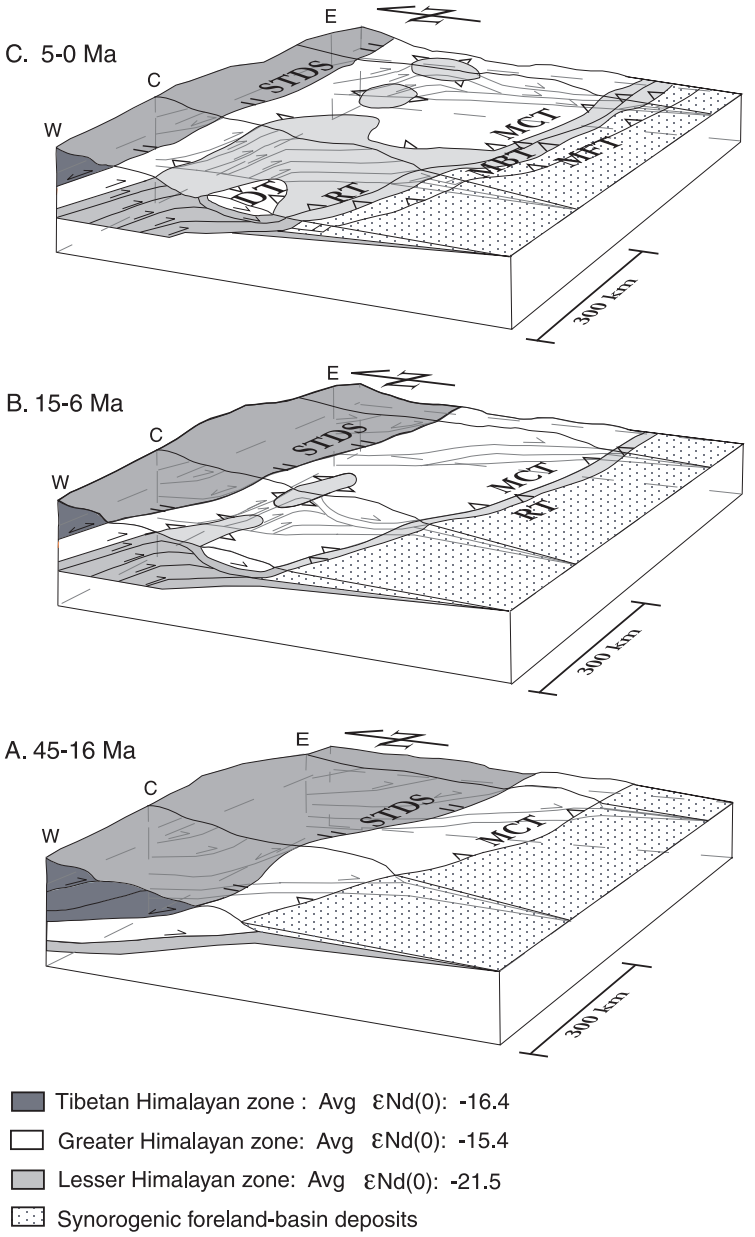

Fig. 6. Interpreted evolution of the Himalayan fold-thrust belt based on $\varepsilon_{Nd}(0)$ values in the Lesser, Greater, and Tibetan Himalayan zones and the synorogenic sedimentary rocks. Caption for Fig. 5 lists the abbreviations. On the left side of each diagram, the positions of the western (W), central (C), and eastern (E) transects are shown (locations given in Fig. 1). The western transect coincides with the Seti and Karnali Rivers and the Khutia Khola data, the central transect with the Trisuli and Kali Gandaki Rivers and the Surai Khola data, and the eastern transect with the Arun River and the Muksar Khola data. The $\varepsilon_{Nd}(0)$ values are from this study only. For all available data, see the bottom of Fig. 4.

this reversal of values by stream capture of Greater Himalayan detritus in the hinterland river system. The $\varepsilon_{Nd}(T)$ values at Surai Khola begin to shift toward −15 at 6 Ma. We interpret this shift to be the result of the Greater/Tibetan Himalayan rocks overwhelming the system, damping the more negative Lesser Himalayan signature. The $\varepsilon_{Nd}(T)$ values at Surai Khola shift to −18 at 2 Ma and then back to −15 at 1 Ma. Again, we interpret these variations as the result of drainage basin reorganization in the hinterland.

The influence of the more negative Nd isotopic signature of the Lesser Himalayan source rocks in the synorogenic sedimentary rocks is subtle. One explanation for why this negative shift may not be as pronounced as expected at the time the Lesser Himalayan sequence was erosionally breached may be that the abundance of REE's is lower in the Lesser Himalayan sequence. Marine carbonates, which make up approximately one-third of the Lesser Himalayan sequence, have lower concentrations of REE's than siliciclastic sedimentary rocks. Thus an equal mixture of detritus derived from Lesser and Greater/Tibetan Himalayan sources would be dominated by Nd from the Greater/Tibetan Himalayan zones. Modern sediment from the Trisuli River in central Nepal yielded an $\varepsilon_{Nd}(T)$ value of −17 (Table 2), which agrees with the inference that the more negative values of the Lesser Himalayan zone are being overwhelmed by Greater/Tibetan Himalayan detritus. The inference that paleo-river systems in the Himalaya were dominated by Greater/Tibetan Himalayan detritus is supported by data from the Bengal fan. The average $\varepsilon_{Nd}(0)$ value since 17 Ma in the Bengal fan is −15 [40,54], which reflects the average values of the Greater/Tibetan Himalayan zones. Coupled with our data from the Eocene and Early Miocene rocks of the foreland basin, this indicates that the Greater/Tibetan Himalayan zones have supplied the majority of the eroded silicate material from the Himalaya throughout the Cenozoic. Despite the dominance of Greater/Tibetan Himalaya detritus since Middle Miocene time, some middle and upper Siwalik foreland basin deposits have fairly negative $\varepsilon_{Nd}(T)$ values (~ -18), which suggests that these transverse drainage systems may be less well-mixed than Bengal fan sediments. Therefore, the influx of sediment with more negative $\varepsilon_{Nd}(T)$ values can be used to identify the time of erosional unroofing of the Lesser Himalayan zone.

5.2. Unroofing/kinematic history

The isotopic data from the synorogenic sedimentary rocks allow us to constrain the unroofing history across Nepal since Middle Eocene time. The schematic three-dimensional diagrams in Fig. 6 represent our interpretation of the Nd isotopic data at 45–16 Ma, 15–6 Ma and 5–0 Ma. The $\varepsilon_{Nd}(T)$ values in the Dumri Formation show a river system dominated by Greater/Tibetan Himalayan detritus from 45–16 Ma (Fig. 6A). These tectonostratigraphic zones were exposed in the fold-thrust belt, actively shedding detritus to be stored in the foreland basin (Figs. 5A and 6A). By Early Miocene time, the Tibetan portion of the fold-thrust belt had already formed, the South Tibetan Detachment system had tectonically unroofed Greater Himalayan rocks, and the Main Central thrust was the front of the fold-thrust belt. The $\varepsilon_{Nd}(T)$ values in the middle Siwalik member show river systems influenced by Lesser Himalayan detritus at 11–10 Ma in western and central Nepal (Fig. 6B). The Greater Himalayan zone had been unroofed in these regions and the Lesser Himalayan zone was exposed by erosional breaching of the growing Lesser Himalayan duplex in the northern part of the fold-thrust belt adding more negative values to the foreland basin deposits (Figs. 5B and 6B). The growth of the Lesser Himalayan duplex passively folded the Main Central thrust sheet and the Greater Himalayan klippen to the south of the duplex along with the overlying Tibetan Himalayan zone (e.g. the Dadeldhura thrust sheet, DT; Fig. 5B). Our data show that the tectonostratigraphic zones within the Dadeldhura thrust sheet have an average $\varepsilon_{Nd}(0)$ value of −14 (Fig. 5B). The $\varepsilon_{Nd}(T)$ values in the middle Siwalik member in eastern Nepal show a river system still dominated by Greater/Tibetan Himalayan detritus at 11–10 Ma. Greater Himalayan rock covered eastern Nepal and supplied the detritus to be stored in the foreland basin. The Ramgarh thrust sheet,

which carries the lower Lesser Himalayan sequence (Kushma and Ranimata Formations and equivalents), marked the front of the fold-thrust belt. The $\varepsilon_{Nd}(T)$ values in the upper Siwalik member at 5–0 Ma show a complex river system in western and central Nepal. Stream capture in the hinterland produced variable $\varepsilon_{Nd}(T)$ values at Khutia and Surai Kholas. Kinematic reconstructions show motion on the Main Boundary thrust at $\sim$5 Ma and motion of the Main Frontal thrust system after 3 Ma (Figs. 5C, 6C; [30]). Muksar Khola in eastern Nepal maintained a steady Greater/Tibetan Himalayan isotopic signature. This suggests that the Arun River Gorge north of the Muksar Khola has only recently exposed rock of the lower Lesser Himalayan sequence, which provides a limited amount of silicate detritus to the system. The unknown in our reconstruction is the extent of the development of the Lesser Himalayan duplex in eastern Nepal. Schelling [23] showed a duplex with two horses. Because we have recently recognized the Ramgarh thrust sheet in eastern Nepal, more mapping is needed to clarify the structural relationships and the character of the Lesser Himalayan duplex.

6. Conclusions

We began this study with two simple questions. Does the Lesser Himalayan zone consistently have more negative $\varepsilon_{Nd}(0)$ values than the Greater Himalayan zone across Nepal? If so, can this difference in Nd isotopic signatures be used in the synorogenic foreland basin deposits to help understand the unroofing history of the Himalaya? We collected Nd isotopic data across an 800 km wide region in the Nepalese part of the Himalayan fold-thrust belt by foot traverses into the mountain range in conjunction with regional mapping. The data have lead us to the following conclusions.

1. The Lesser Himalayan zone has an average $\varepsilon_{Nd}(0)$ value of -21.5. The Greater and Tibetan Himalayan zones have an average $\varepsilon_{Nd}(0)$ value of -16. This difference in $\varepsilon_{Nd}(0)$ values is consistent across Nepal. Combined with previous studies in India, this demonstrates that Nd isotopes are useful as a means of distinguishing between the Lesser and Greater/Tibetan Himalayan zones across most of the Himalaya. This may be important for attempts to understand the kinematics of the so-called Main Central thrust zone.
2. Progressive unroofing of the Himalayan fold-thrust belt is recorded in the Nd isotopic signatures of Eocene–Pliocene synorogenic rocks. Erosion of Lesser Himalayan rock is recorded in the foreland basin by a shift toward more negative $\varepsilon_{Nd}(T)$ values during Middle–Late Miocene time. These data support previous kinematic interpretations of the Lesser Himalayan duplex [5,6,30]. Isotopes in the synorogenic foreland deposits in eastern Nepal are consistent with field observations that indicate that there has been less erosional unroofing in that region.
3. The Nd isotopic signature in the foreland basin system and the Bengal fan is dominated by Greater/Tibetan Himalayan sources. This is because about one-third of the Lesser Himalayan zone is composed of carbonate source rocks, which allows the Greater/Tibetan Himalayan signatures to dominate the Nd isotopic record.
4. The $\varepsilon_{Nd}(0)$ values in the Greater Himalayan zone reveal that the rock is more juvenile than that of the Indian craton, which indicates that it is not Indian basement. These data provide support for previous interpretations that the Greater Himalayan rocks are exotic to India and accreted onto India during the Early Paleozoic.

Acknowledgements

Many thanks to Clark Isachsen and Jeff Vervoot for analytical instruction. John Chesley and Ofori Pearson provided fruitful discussions that improved our understanding of the data. The clarity of this manuscript was improved by reviews from Asish Basu and Scott McLennan. This project was supported by NSF grant EAR-9814060 to P.G.D. and P.J.P. D.M.R. was supported by the Geological Society of America, the

Department of Geosciences at the University of Arizona, and donors to the Geostructures Partnership at the University of Arizona, including BP, Exxon, Conoco and Midland Valley Exploration.*[AH]*

References

[1] A. Gansser, Geology of the Himalayas, Wiley Interscience, New York, 1964, 289 pp.
[2] K. Histatomi, The sandstone petrography of the Churia (Siwalik) Group in the Arung Khola-Binai Khola area, west central Nepal, Bull. Fac. Educ. Wakayama Univ. Nat. Sci. 39 (1990) 5–29.
[3] S. Critelli, R.V. Ingersoll, Sandstone petrology and provenance of the Siwalik Group (northwestern Pakistan and western-southeastern Nepal), J. Sediment. Res. Sect. A 64 (1994) 815–823.
[4] D.A. Pivnik, N.A. Wells, The transition from Tethys to the Himalaya as recorded in northwest Pakistan, Geol. Soc. Am. Bull. 108 (1996) 1295–1313.
[5] P.G. DeCelles, G.E. Gehrels, J. Quade, P.A. Kapp, T.P. Ojha, B.N. Upreti, Neogene foreland basin deposits, erosional unroofing, and the kinematic history of the Himalayan fold-thrust belt, western Nepal, Geol. Soc. Am. Bull. 110 (1998) 2–21.
[6] P.G. DeCelles, G.E. Gehrels, J. Quade, T.P. Ojha, Eocene-early foreland basin development and the history of Himalayan thrusting, western and central Nepal, Tectonics 17 (1998) 741–765.
[7] Y.M.R. Najman, M.S. Pringle, M.R.W. Johnson, A.H.F. Robertson, J.R. Wijbrans, Laser $^{40}Ar/^{39}Ar$ dating of single detrital muscovite grains from early foreland-basin sedimentary deposits in India: Implications for early Himalayan evolution, Geology 25 (1997) 535–538.
[8] Y. Najman, E. Garzanti, Reconstructing early Himalayan tectonic evolution and paleography from Tertiary foreland basin sedimentary rocks, northern India, Geol. Soc. Am. Bull. 112 (2000) 435–449.
[9] S.M. McLennan, S.R. Hemming, D.K. McDaniel, G.N. Hanson, Geochemical approaches to sedimentation, provenance, and tectonics, in: M.J. Johnson, A. Basu (Eds.), Processes Controlling the Composition of Clastic Sediments, Boulder, CO, Geol. Soc. Am. Spec. Pap. 284, 1993, pp. 21–40.
[10] J.D. Gleason, P.J. Patchett, W.R. Dickinson, J. Ruiz, Nd isotopes link Ouachita turbidites to Appalachian source, Geology 22 (1994) 347–350.
[11] A.R. Basu, M. Sharma, P.G. DeCelles, Nd,Sr-isotopic provenance and trace element geochemistry of Amazonian foreland basin fluvial sands, Bolivia and Peru: implications for ensialic Andean orogeny, Earth Planet. Sci. Lett. 100 (1990) 1–17.
[12] R.P. Parrish, K.V. Hodges, Isotopic constraints on the age and provenance of the Lesser and Greater Himalayan sequences, Geol. Soc. Am. Bull. 108 (1996) 904–911.
[13] A. Whittington, G. Foster, N. Harris, D. Vance, M. Ayers, Lithostratigraphic correlations in the western Himalaya - An isotopic approach, Geology 27 (1999) 585–588.
[14] G.E. Gehrels, P.G. DeCelles, J. Quade, B. LaReau, M. Spurlin, Tectonic implications of detrital zircon ages from the Himalayan orogen in Nepal, Geol. Soc. Am. Abstr. Prog. (1999) A374.
[15] P.G. DeCelles, G.E. Gehrels, J. Quade, B. LaReau, M. Spurlin, Tectonic implications of U-Pb zircon ages of the Himalayan orogenic belt in Nepal, Science 288 (2000) 497–499.
[16] T. Ahmad, N. Harris, M. Bickle, H. Chapman, J. Bunbury, C. Prince, Isotopic constraints on the structural relationships between the Lesser Himalayan Series and the High Himalayan Crystalline Series, Garhwal Himalaya, Geol. Soc. Am. Bull. 112 (2000) 467–477.
[17] P. Bordet, M. Colchen, D. Krummenacher, P. Le Fort, R. Mouterde, M. Remy, Recherches geologiques dans l'Himalaya du Nepal: region de la Thakkhola, Editions du Centre National de la Recherche Scientifique, Paris, 1971, 279 pp.
[18] B.C. Burchfiel, L.H. Royden, North-south extension within the convergent Himalayan region, Geology 13 (1985) 679–682.
[19] K.V. Hodges, R.R. Parrish, M.P. Searle, Tectonic evolution of the central Annapurna Range, Nepalese Himalayas, Tectonics 15 (1996) 1264–1291.
[20] T.M. Harrison, F.J. Ryerson, P. Le Fort, A. Yin, O.M. Lovera, E.J. Catlos, A Late Miocene-Pliocene origin for the central Himalayan inverted metamorphism, Earth Planet. Sci. Lett. 146 (1997) E1–E7.
[21] P. LeFort, French earth sciences research in the Himalaya regions: Kathmandu, Nepal, Alliance Française, 1994, p. 174.
[22] J.C. Vannay, K.V. Hodges, Tectonometamorphic evolution of the Himalayan metamorphic core between Annapurna and Dhaulagiri, central Nepal, J. Met. Geol. 14 (1996) 635–656.
[23] D. Schelling, The tectonostratigraphy and structure of the eastern Nepal Himalayas, Tectonics 11 (1992) 925–943.
[24] B.N. Upreti, P. Lefort, Lesser Himalayan crystalline nappes of Nepal: Problems of their origin, in: A. Macfarlane, R.B. Sorkhabi, J. Quade (Eds.), Himalaya and Tibet: Mountain Roots to Mountain Tops, Boulder, CO, Geol. Soc. Am. Spec. Pap. 328, 1999, pp. 225–238.
[25] M.S. Hubbard, T.M. Harrison, $^{40}Ar/^{39}Ar$ age constraints on deformation and metamorphism in the Main Central thrust zone and Tibetan slab, eastern Nepal Himalaya, Tectonics 8 (1989) 863–880.
[26] M.E. Coleman, U-Pb constraints on Oligocene-Miocene deformation and anatexis within the central Himalaya, Marsyandi valley, Nepal, Am. J. Sci. 298 (1998) 553–571.
[27] L. Godin, R.L. Brown, S. Hanmer, High strain zone in the hanging wall of the Annapurna detachment, central

Nepal Himalaya, in: A. Macfarlane, R.B. Sorkhabi, J. Quade (Eds.), Himalaya and Tibet: Mountain Roots to Mountain Tops, Boulder, CO, Geol. Soc. Am. Spec. Pap. 328, 1999, pp. 199–210.

[28] E.J. Catlos, T.M. Harrison, M.J. Kohn, M. Grove, F.J. Ryerson, C.E. Manning, B.N. Upreti, Geochronologic and thermobarometric constraints on the evolution of the main central thrust, central Nepal Himalaya, J. Geophys. Res. (2001) in press.

[29] B.N. Upreti, Stratigraphy of the western Nepal Lesser Himalaya: a synthesis, J. Nepal Geol. Soc. 13 (1996) 11–28.

[30] P.G. DeCelles, D.M. Robinson, J. Quade, T.P. Ojha, C.N. Garzione, P. Copeland, B.N. Upreti, Stratigraphy, structure, and tectonic evolution of the Himalayan fold-thrust belt in western Nepal, Tectonics 20 (2001) 487–509.

[31] H. Sakai, Geology of the Kali Gandaki Super group of the Lesser Himalayas in Nepal, Mem. Fac. Sci. Kyushu Univ. [D] 25 (1985) 337–397.

[32] H. Sakai, Rifting of the Gondwanaland and uplifting of the Himalayas recorded in Mesozoic and Tertiary fluvial sediments in the Nepal Himalayas, in: A. Taira, F. Masuda (Eds.), Sedimentary Facies in the Active Plate Margin, Terra Sci., Tokyo, 1989, pp. 723–732.

[33] P.M. Powers, R.J. Lillie, R.S. Yeates, Structure and shortening of the Kangra and Dehra Dun reentrants, Sub-Himalaya, India, Geol. Soc. Am. Bull. 110 (1998) 1010–1027.

[34] S.G. Wesnousky, S. Kumar, R. Mohindra, V.C. Thakur, Uplift and convergence along the Himalayan frontal thrust of India, Tectonics 18 (1999) 967–976.

[35] J. Lavé, J.P. Avouac, Active folding of fluvial terraces across the Siwaliks Hills, Himalayas of central Nepal, J. Geophys. Res. 105 (2000) 5735–5770.

[36] C. Deniel, P. Vidal, P. LeFort, The Himalayan leucogranites and their probable parent material: The Tibetan slab gneisses, Acad. Sci. Compt. Rend. 303 (1986) 57–62.

[37] C. Deniel, P. Vidal, A. Fernandez, P. LeFort, J.J. Peucat, Isotopic study of the Manaslu granite (Himalaya, Nepal): Inferences of the age and source of Himalayan leucogranites, Cont. Min. Pet. 96 (1987) 78–92.

[38] S. Inger, N.B.W. Harris, Geochemical constraints on leucogranite magmatism in the Langtang Valley, Nepal Himalaya, J. Petrol. 34 (1993) 345–368.

[39] J.A. Massey, Fluid circulation and fault-controlled magmatism in the Central Himalayas, Ph.D. Dissertation, Milton Keynes, UK, 1994, 399 pp.

[40] D. France-Lanord, L. Derry, A. Michard, Evolution of the Himalaya since Miocene time: Isotopic and sedimentological evidence from the Bengal Fan, in: P.J. Treloar, M.P. Searle (Eds.), Himalayan Tectonics, Geol. Soc. (Lond.) Spec. Publ. 74, 1993, pp. 605–622.

[41] A. Michard, P. Gurriet, M. Soudant, F. Albarede, Nd isotopes in French Phanerozoic shales: external vs. internal aspects of crustal evolution, Geochim. Cosmochim. Acta 49 (1985) 601–610.

[42] S.M. Naqvi, J.J.W. Rogers, Precambrian Geology of India, Oxford Monographs on Geology and Geophysics, Clarendon Press-Oxford Press, New York, 1987, 223 pp.

[43] M. Sharma, A.R. Basu, S.L. Ray, Sm-Nd isotopic and geochemical study of the Archean tonalite–amphibolite association from the eastern Indian Craton, Cont. Min. Pet. 117 (1994) 45–55.

[44] D.M. Robinson, P.G. DeCelles, G.E. Gehrels, Contributions of Himalayan and Tibetan upper crustal shortening to thickening of the Tibetan plateau, EOS (2000) 128.

[45] J. Quade, L. Roe, P.G. Decelles, T.P. Ojha, The Late Neogene $^{87}Sr/^{86}Sr$ record of lowland Himalayan rivers, Science 276 (1997) 1828–1831.

[46] T.P. Ojha, R.F. Butler, J. Quade, P.G. DeCelles, D. Richards, B.N. Upreti, Magnetic polarity stratigraphy of the Neogene Siwalik Group at Khutia Khola, far western Nepal, Geol. Soc. Am. Bull. 112 (2000) 424–434.

[47] P.J. Patchett, J. Ruiz, Nd isotopic ages of crust formation and metamorphism in the Precambrian of eastern and southern Mexico, Cont. Min. Pet. 96 (1987) 523–528.

[48] D.J. DePaolo, Neodymium isotopes in the Colorado Front Range and crust-mantle evolution in the Proterozoic, Nature 291 (1981) 193–196.

[49] D.K. McDaniel, S.R. Hemming, S.M. McLennan, G.N. Hanson, Partial resetting of Nd isotopes and redistribution of REE during sedimentary processes: The Early Proterozoic Chelmsford Formation, Sudbury Basin, Ontario, Canada, Geochim. Cosmochim. Acta 58 (1994) 931–941.

[50] E. Garzanti, S. Critelli, R.V. Ingersoll, Paleogeographic and paleotectonic evolution of the Himalayan Range as reflected by detrital modes of Tertiary sandstones and modern sands (Indus transects, India and Pakistan), Geol. Soc. Am. Bull. 108 (1996) 631–642.

[51] K. Arita, Origin of the inverted metamorphism of the Lower Himalaya, central Nepal, Tectonophysics 95 (1983) 43–60.

[52] A. Pêcher, The metamorphism in the central Himalaya, J. Metamorph. Geol. 7 (1989) 31–41.

[53] K.V. Hodges, Tectonics of the Himalaya and southern Tibet from two perspectives, Geol. Soc. Am. Bull. 112 (2000) 324–350.

[54] A. Bouquillon, C. France-Lanord, A. Michard, J. Tiercelin, Sedimentology and isotopic chemistry of the Bengal Fan sediments: The denudation of the Himalaya, Proc. Ocean Drill. Prog. Sci. Res. 116 (1990) 43–58.